

RSC Advances



This is an *Accepted Manuscript*, which has been through the Royal Society of Chemistry peer review process and has been accepted for publication.

Accepted Manuscripts are published online shortly after acceptance, before technical editing, formatting and proof reading. Using this free service, authors can make their results available to the community, in citable form, before we publish the edited article. This *Accepted Manuscript* will be replaced by the edited, formatted and paginated article as soon as this is available.

You can find more information about *Accepted Manuscripts* in the [Information for Authors](#).

Please note that technical editing may introduce minor changes to the text and/or graphics, which may alter content. The journal's standard [Terms & Conditions](#) and the [Ethical guidelines](#) still apply. In no event shall the Royal Society of Chemistry be held responsible for any errors or omissions in this *Accepted Manuscript* or any consequences arising from the use of any information it contains.

Graphene production via Supercritical Fluids

Hanyang Gao, Guoxin Hu*

School of Mechanical and Power Engineering, Shanghai Jiao Tong University, 800 Dongchuan Road, 200240 Shanghai, China.

**hugx@sjtu.edu.cn Tel./Fax: 86-21-34206569*

RSC Advances Accepted Manuscript

Table of contents

Abstract.....	3
Keywords:.....	3
1. Introduction	4
2. Graphene preparation by intercalation-exfoliation of graphite in SCFs.....	6
2.1. Pretreatment of graphite chunk.....	7
2.2. SCFs intercalation	10
2.2.1. Choosing an appropriate SCFs media.....	10
2.2.2. Assistant methods for intercalation	12c
2.3. Exfoliation.....	16
2.3.1. Rapid expansion of supercritical fluid	17
2.3.2. Ultrasonic cavitation exfoliation.....	19
2.3.3. Jet cavitation exfoliation	20
2.4. Intercalation-exfoliation repeat	21
2.5. Characterizations of SCFs graphene	23
2.5.1. Thickness distribution of SCFs graphene.....	23
2.5.2. Size of SCFs graphene.....	24
2.5.3. Quality of SCFs graphene	25
2.6. Advantages and challenges of SCFs intercalation and exfoliation method.....	28
3. Graphene oxide reduction in SCFs	31
4. Concluding remarks.....	33
Acknowledgments.....	34
References.....	35

Abstract

Since supercritical fluids possess the characteristics of low interfacial tension, excellent wetting of surfaces and high diffusion coefficients, they had been employed to intercalate and delaminate tightly-stacked layered materials such as silicates. In recent years, many researchers have begun to explore the possibility of using SCFs as intercalator to penetrate into the nano-gaps of graphite, and exfoliate it into graphene sheets. Although this SCFs intercalation and exfoliation approach is experimentally confirmed to be efficient and promising to produce graphene in large-scale with low-cost, it does not receive the attention it deserves. To arouse interest and reflection on this approach, this review is organized to summarize the recent progress in graphene production by SCFs technology. In this review, the process of SCFs intercalation and exfoliation method is decomposed into three stages, the mechanisms and influence factors for each stage are analyzed, the recommendations for graphene quality improvement are provided, the advantages and challenges of SCFs technology on graphene large-scale production are also summarized. Besides the ability of efficient intercalation, supercritical water or alcohol also can be used as reducing agents to produce reduced graphene oxide from graphene oxide, this SCFs reduction approach is also included in this review.

Keywords: graphene; supercritical fluids; intercalation; exfoliation; reduction.

1. Introduction

In order to meet the needs of applications such as conductive ink, energy storage, conductive plastics, graphene production method requires not only the ability to prepare high quality graphene, but also the potential to be large-scalable and low cost. From this point of view, nowadays, liquid-phase exfoliation (LPE) and graphene oxide-reduction route are considered as two of the most promising methods to mass produce graphene¹. Amazingly, both of the two methods can be implemented in supercritical fluids (SCFs) with high efficiency.

In LPE methods, theoretically, when the surface energy of solvents matches that of graphene, a minimal energy cost of exfoliation is required and the solvent can intercalate into the interlayer of graphite and exfoliate it into isolated sheets². Based on this theory, mono-layer graphene sheets have been successfully directly exfoliated in several solvents, such as N, N-Dimethylformamide (DMF) and N-Methylpyrrolidone (NMP), under ambient pressure by the assistance of ultrasonic irradiation, but the process is time-consuming (several to many days) and low-yielding (usually less than 10%)^{3,4}. Above the supercritical point, fluids possess both “gas-like” and “liquid-like” properties and exhibit a pressure-tunable dissolving power^{5,6}. Because of the low interfacial tension, excellent wetting of surfaces, and high diffusion coefficients, SCFs are expected to be superior solvents to penetrate into the nano-gaps with a high efficiency⁷. Taking advantage of the super penetration ability, SCFs have been utilized to intercalate and delaminate tightly-stacked layered materials such as silicates⁸⁻¹³. In 2007, Gulari and Serhatkulu first suggested using SCFs to delaminate graphite with a coating agent solubilized in a supercritical fluid¹⁴, since then, many efforts were put into this work. Studies confirm that, the penetration and exfoliation speed can be greatly shortened by taking advantage of the super penetration ability of SCFs and the

high-pressure high-temperature environment to dramatically enhance the penetration speed and reduce the reaction time.

Graphene oxide-reduction route involves the completely exfoliation of graphite oxide into individual graphene oxide (GO) sheets^{15, 16} followed by their reduction to produce reduced graphene oxide (rGO) sheets¹⁷. Although many methods were confirmed to successfully reduce GO into rGO^{18, 19}, a method integrating the advantages of efficient, environmentally friendly and low-cost together is still being pursued. Since in supercritical (SC) water, the concentrations of hydrogen ions, which will initiate the dehydration of GO by inter- or intramolecular reactions and cause the reduction of highly strained epoxide groups, decarboxylation and the generation of conjugated p-network, are orders of magnitude higher than those in ambient water, some researchers have attempted to produce rGO sheets from graphite oxide in SCFs treatment by using SCFs reduction ability in recent years. Taking the advantages of quickness, one through put, low-cost and environmental friendliness, SCFs may become a novel and plausible reduction agent to produce rGO in a large scale.

However, despite the noticeable advantages of SCFs methods, the number of published papers focusing on this approach is much less compared to that of oxidation-reduction method, chemical vapor deposition (CVD) method, epitaxial growth method and ball milling method²⁰ etc. Similarly, although numerous reviews have done excellent works on the summary of graphene production and processing, these reports discuss a variety of production methods generally without providing much details on SCFs method. This situation may not only be due to the high temperature and pressure operating environment which makes SCFs approach seem difficult to proceed, but also because currently the quality of result SCFs products still cannot meet the

requirements of practical applications. Therefore, this review is organized to focus on graphene preparation process using SCFs technology and try to help to evoke better ideas on quality improving methods. In this review, the recent progress in graphene production by SCFs technology is summarized by categorizing them into two types, i.e. SCFs intercalation and exfoliation method and SCFs reduction method. In particular, the process of SCFs intercalation and exfoliation method is decomposed into three stages, the mechanisms and influence factors for each stage are analyzed, the recommendations for graphene quality improvement are also provided. Furthermore, the thickness, size and quality of SCFs intercalation and exfoliation graphene are analyzed, the advantages and challenges of SCFs technology on graphene large-scale production are also summarized.

Besides above methods, the excellent mass-transfer property makes SCFs suitable to be used for uniform dispersion nanomaterials onto graphene supporter to produce variable graphene-based composites²¹⁻³³. N-doped graphene sheets can be produced conveniently from N-containing compounds, e.g. ethylenediamine, melamine, hexa-methylenetetramine³⁴, acetonitrile³⁵ or urea³⁶, with graphene oxide/expandable graphite in supercritical environment. Due to the page limitation and the focus of graphene sheets production, these methods are not included in this review.

2. Graphene preparation by intercalation-exfoliation of graphite in SCFs

Typically, SCFs intercalation and exfoliation is the method using SCFs as an intercalator to penetrate, expand and exfoliate natural graphite or its derivatives into graphene sheets. Supercritical density which will be changed by adjusting the temperature, pressure and mass fraction of added solvent, the matching of surface energy between graphene and solvent, and the added external shear force are all considered play a critical role in SCFs exfoliation process^{37, 38}.

For better analysis, the processes of SCFs intercalation and exfoliation method in current studies can be decomposed into three steps: (1) pretreatment of graphite chunk, (2) SCFs intercalation, and (3) exfoliation (Figure 1).

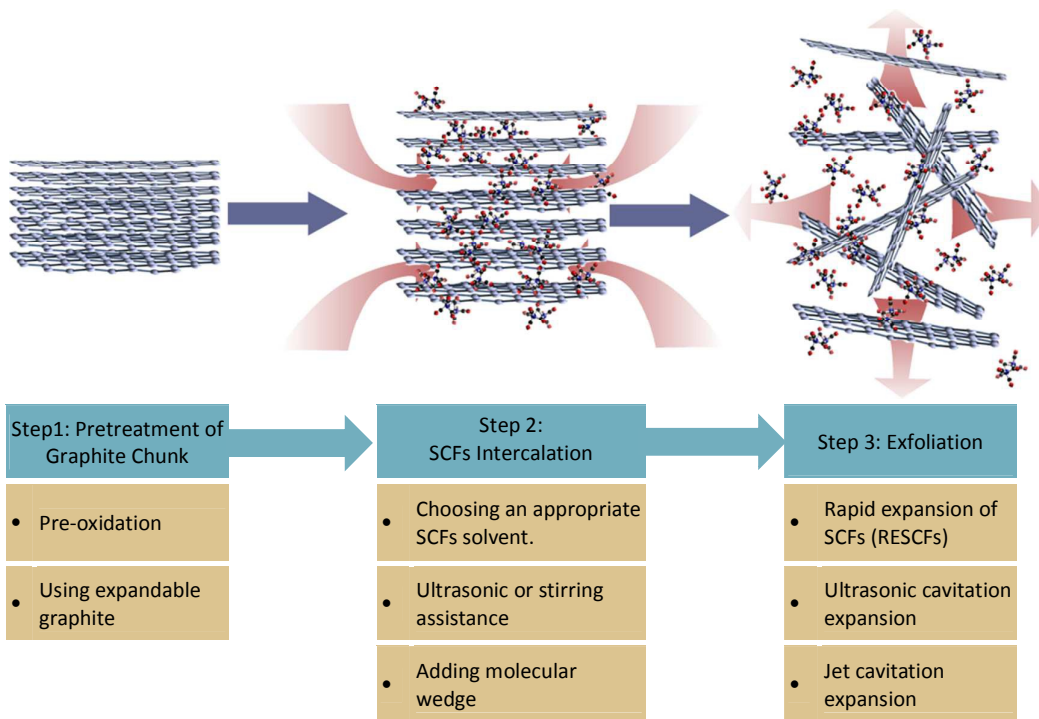


Figure 1. Illustration of three-step stage model of SCFs intercalation and exfoliation method

2.1. Pretreatment of graphite chunk

This is an optional step in SCFs intercalation and exfoliation method, but will directly affect the quantity and quality of the received products.

Graphene sheets can be directly exfoliated from natural graphite crystal using SCFs in a very short time, but the yield of monolayer is generally low. Rangappa and co-workers directly exfoliated natural graphite crystals into high-quality graphene using ethanol, NMP, and DMF as SCFs solvents. Only in a short reaction time of 15 min, natural graphite crystals are exfoliated into sheets. In the final production, about 6–10% are monolayers³⁹. Hu's group has also successfully

exfoliated natural graphite in SC DMF in 15 min, but the yield of monolayer graphene sheets was only 2.5%⁴⁰.

To increase the ratio of monolayer graphene sheets in final products, some research groups tried to use pretreated graphite as starting material. Molecular dynamics studies by Balbuena's group found that the range of interlayer separations for a supercritical carbon dioxide (SC CO₂) molecule being able to diffuse between graphite interlayers is between 5 and 6 Å. Since the separation distance between graphite layers is approximately 3.35 Å, although the distance can be expanded by rotation and twisting of the layers near critical point, the expanded distance caused by the oxygen-containing functional groups should promote the intercalation of SC CO₂⁴¹. Research in Hu's group has showed that using natural graphite which had been slightly treated by nitric acid as a starting material for SC DMF exfoliation could enhance the yield of graphene sheets (3.9%) 1.5 times greater than that from SC DMF exfoliation of natural graphite (2.5%). It is proposed that appropriate amount of polar functional groups attaching on the carbon planes left by nitric acid treatment could facilitate the polar solvent molecules interaction during the SCFs intercalation process and therefor enhance the exfoliation efficiency (Figure 2). Meantime, because the limited number of oxygen-containing functional groups could be easily reduced during the supercritical process, high quality of graphene sheets could be maintained⁴⁰ (see Section 3 for detail in SCFs reduction).

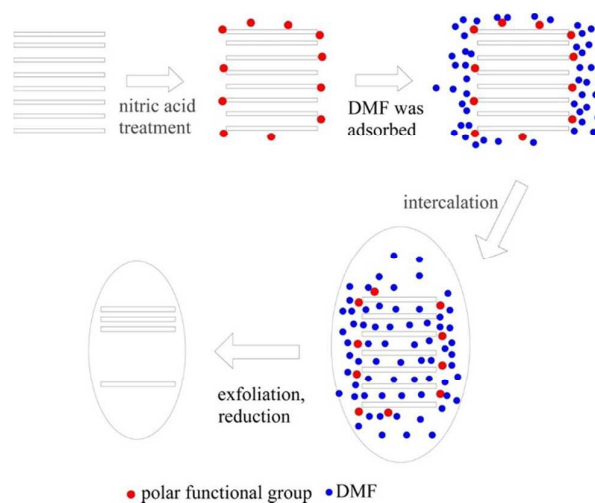


Figure 2. Schematic of the effect of nitric acid treatment on the preparation of graphene sheets by supercritical *N,N*-dimethylformamide exfoliation. With American Chemical Society permission from ⁴⁰.

Expandable graphite is a kind of pretreated graphite. Significant number of polar functional groups anchoring on the carbon planar could evidently enhance the intercalation of DMF molecular, therefore increase the yield of monolayer graphene sheets. Hu's group had used expandable graphite (EG) as starting material to produce graphene sheets. After treated in SC DMF for only 15 minutes, a yield of 7 wt% can be obtained at an optimum condition, much higher than that using lightly nitric acid treated graphite and natural graphite ⁴². But it is also found that, the great number of oxide functional group on expandable graphite could not be fully restored during the SCFs treatment. Therefore, using expandable graphite as a starting material, the yield of monolayer graphene sheets increase but the quality decrease. However, this drawback may give an opportunity to make the graphene manufacturer be able to provide products which meet individual specifications.

In Karimi-Sabet group's study, they reported that the few layers from the top and bottom

sides of graphite flake are more affected by ultrasound waves to generate small gaps by shear forces and cavitation in comparison to the middle layers, since the gaps are the most possible entrances of the solvent molecules in the SCFs step, sonicating big and thick bulk particles into smaller and thinner flakes before the SCFs process will be benefic to the SCFs exfoliation³⁷.

2.2. SCFs intercalation

In this step, SCFs are intercalated into graphite chunk to expand the distance between layers, forming a layer of agent between graphite layers, making graphite swell and get ready for the following exfoliation step. This is a critical step, because successful and adequate intercalation has a direct and important impact on the efficiency of exfoliation, and therefore determine the quality and yield of production.

2.2.1. Choosing an appropriate SCFs media.

In LPE method, interfacial tension between solid and liquid has an important effect on the dispersion degree of a solid when which immersed in a liquid medium⁴³. To graphene, the liquid which can minimize the energy of exfoliation, that is to say, whose solvent–graphene interfacial interaction energy matches that of graphene–graphene, can exfoliate and disperse it. Thus, those possessed surface tensions close to γ -40 mJ m⁻², e.g. *N*-Methyl-2-pyrrolidone (NMP) and isopropanol (IPA), *N,N*-dimethylformamide (DMF) were recognized as the promising solvents. The researchers from different groups confirmed that, using these organic solvents which are also commonly used to disperse carbon materials in ambient environment, can successfully intercalate and exfoliate graphite into monolayer graphene sheets^{39, 40, 44}.

But these solvents have either high boiling point, or toxic effects on human organs. High boiling point limits their viability for real electronic applications, since the presence of remaining

solvent has great impact on the performance of electronic device. Toxic effect enormously increase the difficulty and danger of producing process. Therefore, exfoliation and dispersion graphene in a low boiling point solvent is a preferable route. Luckily, some low point solvent is confirmed to possess similar excellent permeability when above to their SC point. Rangappa and Honma use SC ethanol as intercalator, the yield of exfoliated mono/bilayer graphene in the final products was 10–15%⁴⁵, and the comparison results indicated that no significant difference exists among the quality and layer-number distribution of the products prepared in SC ethanol, SC DMF and SC NMP³⁹. Very recently, Karimi-Sabet's group also successfully exfoliate graphite by using SC ethanol³⁷. In their study, the concept of Hansen solubility parameters was used for analysis of SC exfoliation process, the response surface methodology was also applied to study the effects of process parameters on the exfoliation yield and its optimization.

As the most common SCF agent, SC CO₂ is also used as the supercritical solvent for graphene production because of advantages of its low critical point, non-toxicity, low cost and environment friendliness⁴⁶. Both computational and experimental approaches have been developed to study the exfoliation process. In computational studies, Balbuena's group used molecular dynamics to study the graphite exfoliation using SC CO₂, results showed that the pressure effect seemed to have a larger effect on the exfoliation than the temperature⁴¹. Yang and Wu simulated the potential of mean force between two graphene nanosheets in SC CO₂ for the study of colloidal dispersion stability of nano-sized graphene sheets in SCF media. The results indicated that the free energy barrier between graphene sheets in the SC CO₂, which induced by the single-layer confined CO₂ molecules, can possibly obstructing the aggregation of graphene. Therefore, the density of SC CO₂ plays an important effect on the graphene stability, since at

higher SC CO₂ fluid density, there are more confined CO₂ molecules within the interplate regions, resulting in a stronger repulsive free energy barrier⁴⁷.

In experimental studies, Zhao's group used SC CO₂ to intercalate and exfoliate natural graphite, results showed that the SC CO₂ process alone cannot independently exfoliate graphite into single- or few-layer graphene, only sheets with more than ten layers of graphite are formed in SC CO₂⁴⁸. Ger's group immersed natural graphite in SC CO₂ with a treatment at 100 bar and 45 °C for 30 min, typical thickness of the final products is about 10 atomic layers⁴⁹. Park's group showed that SC CO₂ can intercalate expandable graphite, but the repeat of SC CO₂ process is needed to reduce the layer numbers of the products⁵⁰. It seems that, while ethanol, DMF and NMP can be used as appropriate supercritical agents to accomplish a sufficient penetration, and exfoliation of graphite into mono/bilayer graphene sheets, SC CO₂ alone is insufficient to completely exfoliate graphite into monolayer graphene sheets. The limited intercalation ability may not only due to the nonpolar nature, but also to its small molecular size which leading to a secondary escape of the inserted ones. However, some assistant methods (listed in 2.2.2.) can optimize the permeability and promote the penetration efficiency.

Most recently, Karimi-Sabet's group reported that theoretical measurements of Hansen solubility parameters (HSPs) indicated that the exfoliation efficiency is more higher at the supercritical condition in which the HSPs of solvent are close to that of graphene³⁷. This results may be a guide in future for choosing an appropriate solvent for SCFs graphene production.

2.2.2. Assistant methods for intercalation

The features of low interfacial tension, excellent wetting of surfaces, high diffusion coefficients and outstanding power of solvation make SCFs a superior solvent for the rapid

penetration of all the interlayers of graphite. Comparing with the intercalation under ambient environment, SCFs intercalation obviously shorten the processing time and increase the effectiveness. To maximize the advantage of SCFs, researchers have explored to promote the intercalation extent using other methods, such as ultrasonic or stirring assistance and adding molecular wedge (Figure 3).

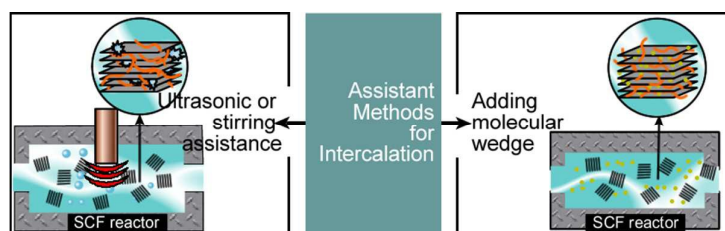


Figure 3. Methods to promote the intercalation extent: ultrasonic or stirring assistance and adding molecular wedge.

2.2.2.1. Ultrasonic or stirring assistance

During ultrasonic cavitation, when cavitation bubbles collapse, high-speed liquid microjets are generated and will act as a solvent micropump that can force a solvent into the interlayer of graphite, it can be expected that the microjets with high pressure shock waves would influence the mass transport between the narrow gaps⁵¹. Zhao's group coupled the technique of SC CO₂ with ultrasound to prepare graphene sheets. They found that although SC CO₂ process or ultrasound process cannot exfoliate graphite into single- or few-layer graphene independently, the approach of coupling ultrasound to SC CO₂ can produce single- and few layers graphene sheets. They found the effect of ultrasonic cavitation in SC CO₂ help to weaken the van der Waals interplanar interactions of graphite, therefore enhance the intercalation of SC CO₂, and ultimately improve the exfoliate efficiency⁴⁸. They demonstrated that both ultrasonic treatment time and ultrasonic power have great impact on the yield of product. The graphene sheets were obtained with 24% as

monolayers, 44% as bilayers, and 26% as trilayers under the optimum condition ⁴⁶.

Shear stress induced by stirring will also provide a wedging force to facilitate the intercalation of solvent into the interlayer of graphite. Park's group used stirring to enhance the penetration and exfoliation efficiency of SC CO₂ system. They demonstrated that SC CO₂ with no or short stirring time (10 min) was ineffective to produce graphene sheets, however, higher pressure and longer stirring time would lead to more exfoliation of graphite bunk. They found that the high pressure can enhance the role of stirring in penetration promoting, under a higher pressure, a short stirring time can effectively facilitate intercalation, while a longer stirring time is required under a smaller pressure to achieve the same extend of exfoliation ⁵⁰. Li and Liu's group also found that the fluid rotating speed has important effect on product yield in SC CO₂ process. A high fluid rotating speed of 2000 r/min can enhance graphene yield obviously from 10% (without stirring) to 70% ⁵². According to this study, SC CO₂ molecules can invade into the interlayers of graphite by the assistance of high-speed fluid shear stress which applied by stirring, the exfoliation efficiency will be enhance under the fierce turbulence and the lateral striking of stirring SC CO₂ molecules.

2.2.2.2. Adding molecular wedge

Some researchers found that pyrene and pyrene-derivatives can be used as a “molecular wedge” to promote the penetration of SCFs. Rangappa and Honma showed that the presence of 1-pyrene sulfonic acid sodium salt in the *in-situ* exfoliation reaction by SC ethanol could efficiently increase mono/bilayer graphene sheets yeild to about 60%. This is a 4-times higher yield than that of graphene sheets exfoliated in the absence of any modifier under a similar SCFs process ⁴⁵. The research of Xu's group also indicated that the exfoliation of graphite using SC CO₂

could be obviously enhanced by adding pyrene-derivatives as molecular wedge^{53, 54}. They claimed that pyrene-polymers exhibit poor native solubility in CO₂ which causes the pyrene-polymers to become increasingly less soluble and attempt to minimize their interaction with CO₂, find their way to the graphite interlayers that act as molecular wedges, and form a large number of p-p stacking interactions with the conjugated p-network of graphene sheets. During this process, SC CO₂ acts as penetrant, expanding agent and antisolvent, and the pyrene-polymer acts as molecular wedge and modifier. Both pyrene-polymer and SC CO₂ play essential roles in obtaining stable solution of graphene sheets (Figure 4). They also found the molecular weight of pyrene-polymers, *pyrene-polyethylene glycol (pyrene-PEG)* and *pyrene-polycaprolactone (pyrene-PCL)*, and the solvent system have significant influence on exfoliation results. Only a polymer with suitable molecular weight could be used as a wedge to intercalate graphite interlayer, because the polymer with a higher molecular weight may be hard to insert into the graphite interlayers due to the limited space within the interlayer. Recently, Xu's group demonstrated that graphite powder can be efficiently exfoliated into monolayered and few-layered nanosheets based on the driving forces originating from micelles to reverse micelles in the emulsion microenvironment built by SC CO₂ with suitable surfactant⁵⁵.

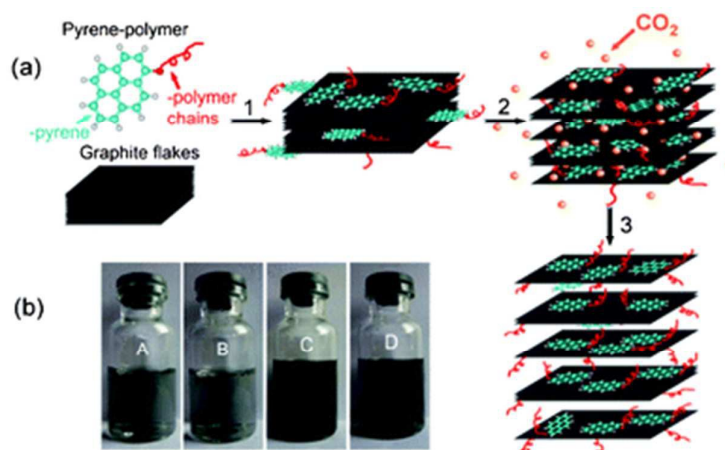


Figure 4. (a) Schematic illustration of the preparation process of pyrenepolymers functionalized graphene sheets based on SC CO_2 's assistance (from step 1 to step 3). (b) Photographs of pyrene-PEG2K functionalized graphene aqueous dispersion (A), pyrene-PEG5K functionalized graphene aqueous dispersion (B) pyrene-PCL19 functionalized graphene dimethylsulfoxide (DMSO) dispersion (C) pyrene-PCL48 functionalized graphene DMSO dispersion (D). With Royal Society of Chemistry permission of⁵³.

2.3. Exfoliation

After adequate penetration of SCFs between the adjacent interplanar of graphite achieved in the intercalation step, exfoliation step is followed to accomplish the task of producing high quality graphene sheets with high monolayer ratio. Although a small part of graphene sheets are estimated to be peeled off from graphite in the intercalation step, the main part of the exfoliation work will take place in this step.

In the published studies focusing on graphene production by SCFs, three methods were used to exfoliate graphene sheets from the intercalated graphite: rapid expansion, ultrasonic cavitation and jet cavitation (Figure 5). While the former method is using rapid expansion of SCFs

intercalator between the interlayers of intercalated graphite to realize exfoliation, the latter two methods strengthen the efficiency of exfoliation by cavitation.

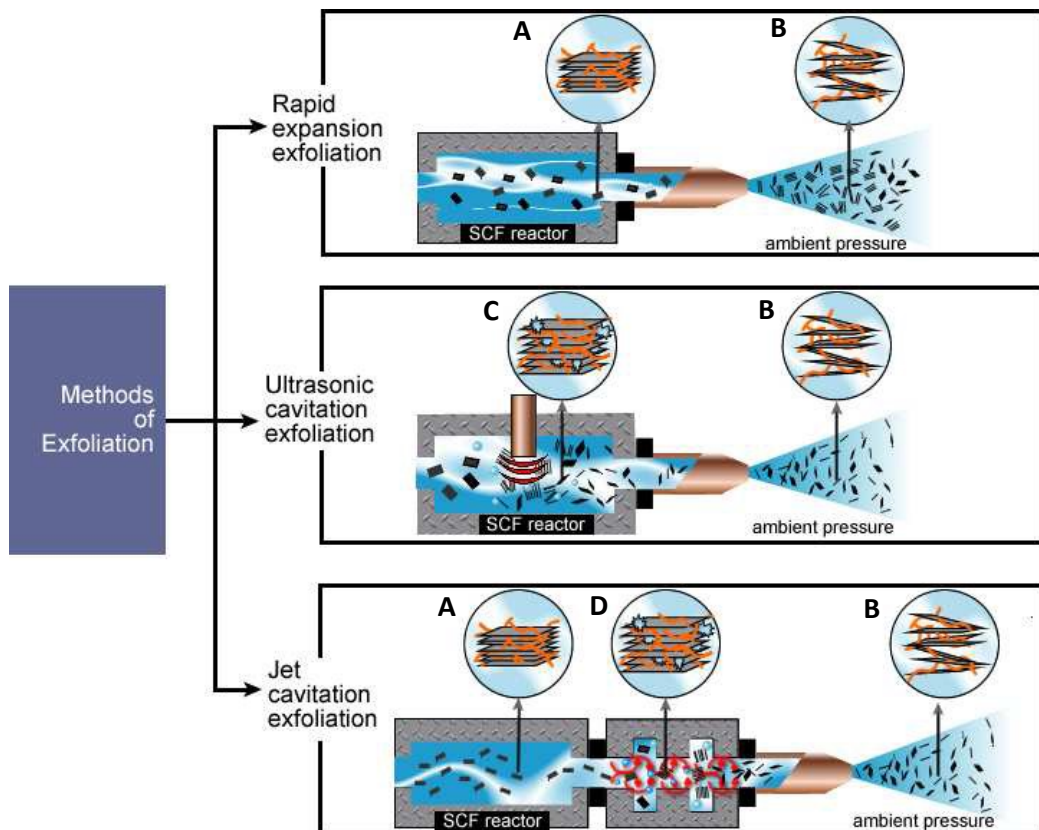


Figure 5. Methods of exfoliation: rapid expansion, ultrasonic cavitation expansion and jet cavitation expansion. The latter two methods strengthen the efficiency of exfoliation by cavitation. A: graphite intercalated by SCFs. B: intercalated graphite exfoliated into graphene after rapid expansion. C: the thermal shock injection and high vapor pressure created by ultrasonic cavitation in the microenvironment act on the intercalated graphite and induce exfoliation. D: the micro-jets and shock waves generated by jet cavitation act on the intercalated graphite and induce exfoliation.

2.3.1. Rapid expansion of supercritical fluid

In process of thermal exfoliation of graphite oxide, the oxygen-containing functional groups between the graphite layers are vaporized at a high temperature, and forming a pressure in the

interlayer. Large pressure difference between the inner layer and the outer layer of graphite causes the exfoliation of material⁵⁶. Similarly, during the SCFs intercalation step, graphite is expanded by SCFs intercalation reagents which penetrate between the graphite layers and remain as stable species. When exposed to an abrupt decrease in pressure, the intercalation compounds decompose into gaseous products, resulting in a large pressure difference between inner layer of graphite and ambient environment. This large pressure difference evokes enough force to push apart graphite basal planes along the “c” axis direction, with the result of an increase in the volume of the graphite of up to 300 times, a lowering of bulk density, and approximately a 10-fold increase in surface area⁵⁷.

Rapid expansion method, which means relieving the pressure quickly, can be conveniently realized by quickly opening the valve connected to the SCFs reactor or spraying through a nozzle into an atmospheric vessel. The instantaneous expansion of SCFs during an abrupt depressurization step is the key factor to the success of exfoliation. Zhao's group produced graphene sheets by spraying SC CO₂ intercalated graphite into a beaker^{46, 48}. Shieh and his co-workers investigated the effect of depressurization rate on interlayer expansion of layered montmorillonite clay, results showed that the slower depressurization rate leads to a smaller interlayer spacing in layered material, which suggested a beneficial effect of high speed depressurization on the interlayer distance expansion of layered materials⁵⁸. Park's group depressurized the SC CO₂ reactor by rapidly opening the vent valve, found it is the sudden expansion of CO₂ molecules, which were intercalated between EG layers, that cause the exfoliation of the expansion graphite into graphene sheets⁵⁰. Ger and co-workers also reported that the SC CO₂ intercalated graphite was forced to exfoliate or delaminate by the expansion of the

SC CO₂ disposed interstitially between the layers upon rapid depressurization of the vessel. In their experiment, the depressurization was performed by opening a blow-off valve and the gas was released at a rate of about 40 mL/s. They claimed that compared to the conventional chemical oxidation and exfoliation approach, where the exfoliation is caused by thermal expansion of the gases trapped between the graphene sheets, this method offers a much faster expansion mechanism, and thus a stronger force to push the adjacent layers apart⁴⁹.

2.3.2. Ultrasonic cavitation exfoliation

Upon exposure to ultrasonic irradiation, the high-speed liquid microjets induced by ultrasonic irradiation will serve as nanoscale chisels, continuously attack and wedge into the intercalated graphite to loose and peel it. Since the intensity of the released energy is limited by the cavitation threshold, to maximize the energy stored within the resonant system, the cavitation must be suppressed. Gaitan and Kenneth^{59, 60} found that the inertial cavitation threshold was linearly dependent on the static pressure, and cavitation can be suppressed by increasing the static pressure of the fluid. When static pressure was under 30MPa, the energy released from transient cavitation increases with the increasing in static pressure of the fluid. Compared with the normal temperature and pressure conditions, the relative intensity of cavitation increases an order of magnitude. It is reasonable to deduce that the high pressure up to ~GPa and the high shear stress up to ~MPa induced from cavitation under high pressure, will benefit the exfoliation efficiency of graphene.

During ultrasonic cavitation exfoliation, thermal shock injection and high vapor pressure created by ultrasonic cavitation in the microenvironment act on the bulk material and induce exfoliation⁶¹. Although ultrasound at atmospheric pressure baths cannot produce sufficiently intensive cavitation to provide graphite-delamination without chemical agents, an intensive

cavitation field in a pressurized reactor has a high enough level of intensity for efficient graphene exfoliation⁶². Because the graphite is already well intercalated and swelled by SCFs, as a strengthening method, ultrasonic cavitation can obviously enhance the exfoliation efficiency of rapid expansion. In common LPE method, unintercalation graphite is sonicated in solvents at ambient condition, dozens of days are needed to obtain a small amount of graphene sheets; while in SCFs ultrasonic cavitation exfoliation method, by using SCFs-intercalated graphite and high-pressure sonication, the required time can be successfully shorten to few hours.

2.3.3. Jet cavitation exfoliation

Hydrodynamic cavitation has been increasingly used as a substitute to conventional acoustic cavitation for process intensification owing to its easy and efficient operation. Hydrodynamic cavitation is caused by the pressure variation in a flow. The force generated by jet cavitation has been confirmed to be effective in exfoliating crystal graphite into graphene sheets. Shen's group found that when jet cavitation-generated bubbles collapse, micro-jets and shock waves act on the graphite surfaces instantly, resulting in compressive stress waves. Once compressive stress waves spreading to the free interface of graphite, a tensile stress wave will be reflected back to the graphite body. Since the energy of tensile stress (around several kpa) is much higher than the interlayer binding force of layered graphite, graphite can be exfoliated into graphene effectively⁶³. Therefore, micro-jets may split graphite flakes just as a wedge is driven into the interlayer. Meanwhile, turbulence, viscosity, and particle-particle collisions induced shear force can result in bulk materials self-exfoliation down to single or few layers through their lateral self-lubricating ability (Figure 6)⁶⁴.

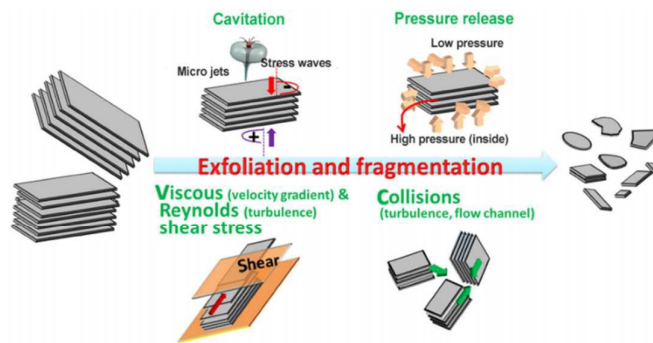


Figure 6. Schematic of the exfoliation mechanism of the fluid dynamics route for production of graphene and its analogues. With springer permission from ⁶⁴.

2.4. Intercalation-exfoliation repeat

The repeat of intercalation-exfoliation steps can strengthen the efficiency of SCFs method. Although the quality of graphene sheets produced by one-pass SC CO₂ treatment is unsatisfactory, some researchers found that repeat of SC CO₂ treatment can further reduce the layer number of the products. Parks group showed that 47% of the products made of one-pass SC CO₂ treatment were consist of 6-8 layers, while 35 % products which received secondary SC CO₂ treatment had 3-5 layers and 8% had 1-2 layers ⁵⁰. Zhao's group also indicated that the yield of graphene sheets produced in SC CO₂ can be easily raised to about three times higher by simply repeated exfoliation of the sediment remained in the reactor at the same operating parameters ⁴⁶.

Procedures can easily be repeated for many times in a continuous-flow-type reactor system. With Figure 7, the device diagram, the repeated process can be clearly shown (taking ultrasonic-assistant SCFs treatment for an example): After intercalated by SCFs in SCFs reactor with the assistance of ultrasonic wave, swollen graphite is sprayed to vessel to achieve exfoliation by rapid expansion. While the qualified products can be collected through "exfoliated products output", the unexfoliated ones are pumped back to SCFs reactor to undergo a new round of

intercalation process. The recycle of intercalation and exfoliation can be repeated for many times until all the final products meet the acquirement.

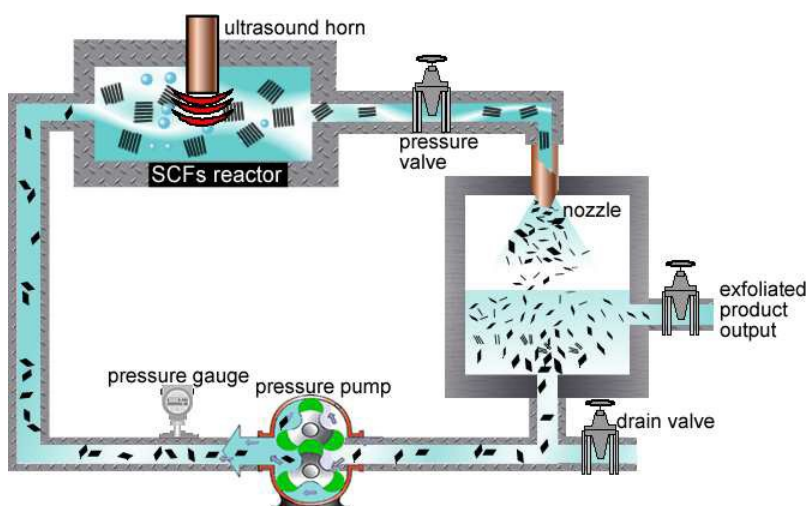


Figure 7. Flow diagram of graphene production by repeated ultrasonic-assisted SCFs treatment: swollen graphite is sprayed to vessel to achieve exfoliation by rapid expansion after intercalated by SCFs in SCFs reactor with the assistance of ultrasonic wave. The qualified products can be collected through exfoliated products output, and the unexfoliated ones are pumped back to SCFs reactor to undergo a new round of intercalation process.

The studies by Honma's group indicated that, even without the above spraying-reloading circulation, exfoliation efficiency can be obviously enhanced by simply intermittently heating and cooling the SCFs reactor for several times⁶⁵. In their study, both continuous heating protocol and intermittent heating protocol were carried out with keeping the reactor in the furnace for a same total duration. During the reaction, the heating and cooling processes were repeated six times intermittently in intermittent heating protocol while the temperature was kept stable in the continuous heating protocol. AFM and Raman analysis indicated that, intermittent heating can further enhanced the exfoliation and simultaneous cutting processes, bringing the decreases both

in thickness and lateral size of the nanographene products.

2.5. Characterizations of SCFs graphene

2.5.1. Thickness distribution of SCFs graphene

Generally, two kinds of methods are used to calculate the thickness distribution of SCFs graphene products: Raman and AFM. Honma's group precisely identify the number of layers from the shape and position of the 2D band in the Raman spectra. They had systematically identified 1–10 layers of graphene sheets in their exfoliated graphene powder samples. For each sample, hundreds of spots were measured from several different regions with regular spacing to count the number of layers. The results are presented as histograms and are used to determine the degree of the exfoliation in each samples^{34, 39, 45, 65, 66}. Xu's group and Park's group calculated the graphene layers distribution based on the AFM measurements of 100~150 graphene nanosheets which were randomly selected. A histogram of layer number distribution was obtained from the results for exhibiting the exfoliation efficiency^{50, 54}. Zhao's group calculated the layer distribution both by AFM and Raman and confirmed that two results are roughly consistent⁴⁶. Layer distribution and the corresponding calculation method of some SCFs graphene production sample are listed below in Table 1 for an overlook and comparison.

Table 1 Calculation method and layer distribution of SCFs graphene products

	samples	starting material	SC media	assistantc	calculation method	layer distribution
1	GSS ref. ³⁹	graphite,	NMP, DMF, EtOH	none	Raman	90–95% <8 layers with a 6–10% monolayer yield.
2	G-PA ref. ⁵⁴	graphite	CO ₂	pyrene-derivatives in DMF	AFM	82% < 3 layers with a 6% monolayer yield.
3	graphene ref. ⁴⁶	graphite	CO ₂	ultrasonic	AFM and Raman	94% < 3 layers with a 24% monolayer yield, a 44% bilayer yield and a 26% trilayer yield.
4	imGNS ref. ⁴⁵	graphite	EtOH	1-pyrene sulfonic acid sodium salt (1-PSA)	Raman	60% ≤ 2 layers with a 37.5% monolayer yield.
5	GNS ref. ⁵⁰	expanded graphite	CO ₂	none	AFM	47% ≤ 8 layers with a 3% monolayer yield.

2.5.2. Size of SCFs graphene

It should be noted that, when observed with AFM, the morphology of SCFs graphene sheets showed an obvious difference compared with those produced by other methods (Figure 8). Firstly, the diameter of exfoliated flakes is small, which is around tens to hundreds of micrometers; secondly, the typical shape of SCFs graphene is irregular round instead of angular. Although current study has not provided an explanation for this phenomenon, the unique environment of high pressure and temperature, as well as liquid reaction medium of SCFs should be the cause ⁴⁸.

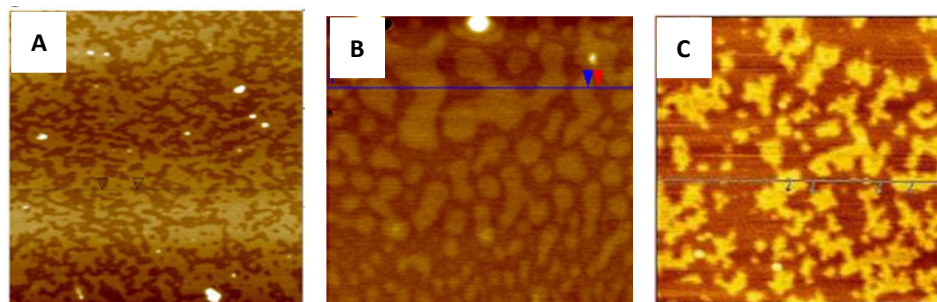


Figure 8 AFM images of graphene sheets produced (A) in SC DMF. With Elsevier permission from ⁴² (B) in SC EtOH with water as co-solvent. With Elsevier permission from ³⁷ (c) in ultrasonic-assisted (300W) SC CO₂. With Elsevier permission from ⁴⁸.

Small size makes SCFs graphene more “rigid” than the flexible big-size ones made by other methods and therefore avoiding the wrinkles, and also increases the dangling bonds at the edges of sheets. Their “rigidness”, rich dangling-bonds and two dimensional morphology make them have the tendency to assemble together in an edge-by-edge mode ⁶⁷, and form a film-like structure ⁶⁸ on the substrates (Figure 8a).

Although the barriers which may hinder electron mobility are increased in this splicing film, considering the high quality of SCFs graphene sheets and the convenience of making film, SCFs graphene may become a promising candidate to produce graphene-based films in an industrial scale. However, the small sheet size will also limit the usage of SCFs graphene in the area such as catalyst substrate, mechanical strength enhancement etc. The full and sufficient intercalation before exfoliation maybe the key to produce large size graphene sheets under SCFs route.

2.5.3. Quality of SCFs graphene

The quality of graphene is very important for its applications. The defective sites, the edge state, inter-sheet boundaries and on the basal plane degrade the performance not only in catalyst and

mechanical strength enhancement, but also in thin film transistor and transparent conductive film. One of the advantages for the graphene produced by SCF exfoliation is high quality without introducing defect and functional group during exfoliation process. To characterize the quality of SCFs graphene sheets, Raman, X-ray photoelectron spectroscopy (XPS) and IR are commonly used.

In the most cases, D-band can usually be observed in Raman spectrum of SCFs graphene sheets, however, the intensity is low and the value is similar to that of highly purified single wall carbon nanotubes, indicating that SCFs do not induce defects on the graphene plane during the exfoliation process, and the D-bands are mainly due to edge effects^{40, 45, 53, 54}. The ratios of the intensities of D-band and G-band peaks (I_D/I_G) are commonly ranged from 0.02 to 0.23, which is much lower than the reduced graphene oxide (around 0.80~1.10). In FTIR spectrum, SC CO₂ graphene has similar FTIR patterns with initial graphite⁴⁶. The absence of C–OH peak and –COOH peak⁴⁰ indicated that no oxygen-containing groups or any extra groups were introduced during the SCFs exfoliation process. In the XPS spectra of SC CO₂ graphene, the main C–C peak makes up from 81% to 93% of the spectrum, only weak C–O peak can be found at 286.3 eV. High degree carbon to oxygen (C/O) ratio can also confirm the low levels of oxidation and the high quality of the SCFs exfoliated graphene sheets⁵³. From all the evidences from Raman, FTIR and XPS, it can be concluded that no extra oxygen-containing groups are induced on the carbon plane during the SCFs process and there are no significant defects on the SCFs graphene sheets, the quality of these graphene sheets are quite high.

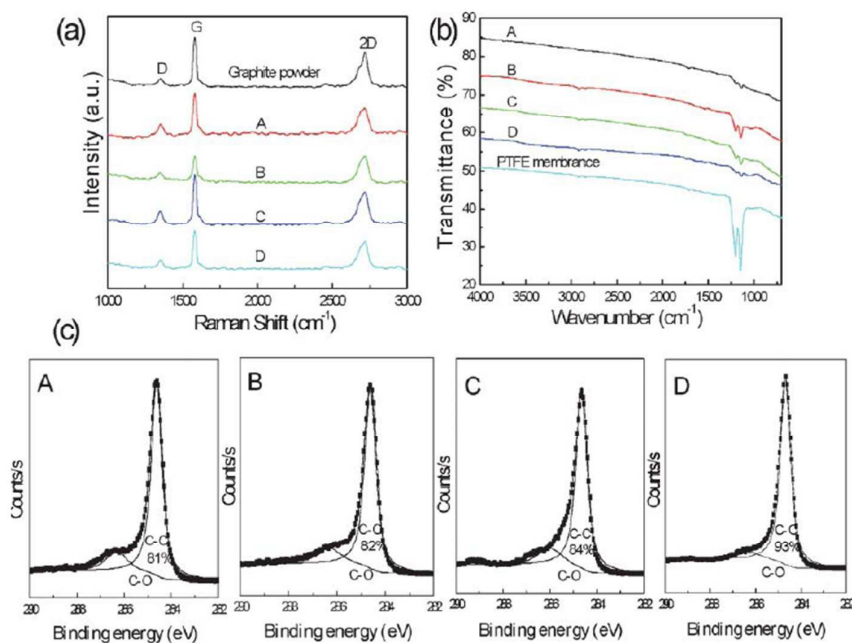


Figure 9 (a) Raman spectra of graphite powder and four vacuum filtered graphene films, which were prepared by non-covalent functionalization of pyrene-PEG2K (A), pyrene-PEG5K (B), pyrene-PCL19 (C) and pyrene-PCL48 (D), respectively. (b) ATR-FTIR spectra of pure PTFE membrane and four vacuum filtered graphene films (A–D) (c) Carbon 1s core-level XPS spectra for four vacuum filtered graphene films (A–D). The Shirley background has been removed. Fit lines represent graphitic carbon (C–C ~284.6 eV), and C–O (~286.3 eV). With Royal Society of Chemistry permission from ⁵³.

High quality structure is expected to endow SCFs graphene good conductive properties. Zhao's group compared the electrical conductivity of the ultrasonic-assistant SC CO₂ graphene film with that of GO film graphite film. Results indicated that the σ_{DC} of SCFs graphene film with thickness of 300 nm (2.8×10^7 S/m) is high as that of the film prepared by CVD method, and is two orders of magnitude higher than that of the graphite film with same thickness (2.5×10^5 S/m), three orders of magnitude higher than that of the annealed reduced GO film ⁴⁶. Honma's group

investigated the current–voltage (I–V) characteristics of individual multilayer graphene sheets prepared in SC EtOH, DMP or DMF media. Typical I–V curves showed that the resistances of SCFs graphene sheets (in the range of 2–6 k Ω), are much lower than that of their counterparts which produced by other chemical approaches³⁹. Li and Liu's group measured the electrical conductivity of the film made from graphene prepared in SC CO₂ shear-assisted exfoliation. The film also showed a high conductivity of 4.7 $\times 10^6$ S/m⁵². It is foreseeable that the good conduction and electron-carrier capacity which endowed by the defect-free and unoxidized characterization would make SCFs graphene sheets a promising candidate for the ultra-high speed transistors or photodetectors in modern nanoelectronic devices.

2.6. Advantages and challenges of SCFs intercalation and exfoliation method

Comparing with other graphene production methods, SCFs intercalation and exfoliation method integrates many advantages together, making it a promising approach to realize graphene large-scale and low-cost production. However, to achieve this goal, a number of technical problems must to be overcome. In the following paragraph and Table 2, the advantages and challenges of SCFs intercalation and exfoliation method are summarized and listed.

Advantages. (1) In this approach, graphene is directly exfoliated from graphite, the defects or oxides in the resulting products are much less than those prepared from chemical oxidation-reduction approach; (2) It is an efficient approach, SCFs can penetrate into the interlayer of graphite with high efficiency, reducing intercalation and exfoliation time from days to hours, even to minutes. It is also an up-scalable approach, offering possibilities towards large-scale industry continuous production and automation; (3) Products are diversified, both graphene powder and graphene dispersion can be obtained by choosing a proper supercritical media (e.g.

adjusting the ratio of SC CO₂ with organic solvents). Graphene suspension can be used to deposit graphene conveniently in a variety of environments and on different substrates⁶¹; (4) Process is flexible, surface modifiers or additives can be easily added in the reaction system at a certain stage to change the property, or to avoid the re-stack of graphene product, or to synthesize graphene-based composite materials; (5) It is an environmental-friendly approach, avoiding the use of highly toxic or hazard materials.

Challenges. (1) One of the main challenges of this method is to separate unintercalated or unexfoliated graphene from the qualified products. Currently, continuous separation of nano-scale materials with high throughput is still a tough task. (2) Since the size of SCFs graphene sheets is small, their role as catalyst substrates or mechanical strength-enhancing additives are limited. Full and sufficient intercalation before exfoliation may be the key to produce large size graphene sheets in SCFs route. (3) The high initial investment in SCFs equipment may limit the widespread use of this method.

Table 2

Summary of advantages and challenges associated with SCFs graphene production route

Advantages	Challenges
• high quality graphene production with good conductivity	• small size of graphene sheets
• high efficient, large-scale continuous production	• high investment in equipment
• diversified production, both graphene powder and graphene dispersion can be obtained	• separation of unintercalated graphene from production.
• flexible, an additive can be easily added in reaction system to produce graphene-based composite materials	
• environmental-friendly	

Currently, chemical oxidation-reduction method and SCFs technique are two most potential methods to realize rGO/graphene large-scale industrial production. Chemical oxidation-reduction method has low entry barrier, the monolayer ratio of rGO products are relatively high. Although the *sp*² carbon network cannot be totally restored during the reduction process, the oxygen containing functional groups anchoring on the carbon planes can be used as binding sites to form composite materials with other compounds. Therefore, chemical oxidation-reduction has become the most commonly used method in laboratory research. Recently, commercial products prepared by this method have appeared in the market. In comparison, complicated equipment and high temperature high pressure operating environment increase the entry barriers of SCFs method, but the stable product quality derived from continuous producing process, high electrical conductivity derived from direct graphite exfoliation, and no need to deal with the waste...also make it an attractive method to achieve the large-scale industrial production. Table 3 is the summarized list to make a clear comparison between these two methods from technical and economic point of view.

Table 3

Technical and economic comparison of chemical oxidation-reduction method and SCFs technique

	Chemical Oxidation-Reduction Method	SCFs Technique
Process Characteristics	Batch production. Processes involving three steps: oxidization & intercalation, exfoliation by external force and product separation	Automatically continuous production. Production concentration and separation is easy to be achieved by releasing SC CO ₂
Production cycle	time-consuming	a few hours
Raw material consumption	graphite, water, strong acid, strong oxidant, reducing agent	graphite, water, CO ₂ (can be recycled)/other SCFs, surfactant
Equipment investment and maintenance	ordinary	slightly higher, 1.0~1.5 times higher than chemical oxidation-reduction method

Number of production staff	more than SCFs technique owing to the batch production process	relatively fewer
Production waste	high cost to treat the oxidizing agent in concentrated sulfuric acid, and high toxic reducing agent	Environmental friendly, nearly no waste produced
Products feature	rGO with defects and low electrical conductivity	graphene with relatively small size, less defects and high electrical conductivity
Market price	high price for high quality products with layers less than three	having potential to lower the price

3. Graphene oxide reduction in SCFs

Owing to the simplicity, economical feasibility, scalability and allowing versatile adaptation of chemical functionalities, chemical reduction method has become one of the most popular approach to produce rGO. In a typical process of chemical reduction method, pristine graphite is first oxidized to graphite oxide and afterward reduced to rGO sheets. However, the main obstacle of this route is the difficulty to find an efficient and environmentally friendly reducing agent. Hydrazine, which is the most commonly used reducing agent, is highly toxic and dangerously unstable, making it unattractive for use in large-scale production; whereas, other “green” reductants suggested by researches, usually obtain their non-toxic feature at the expense of losing active reducing power, and cannot restore the structural defect on carbon planar completely. Therefore, there is an urgent need to find an environmentally-friendly, cheap and effective reducing agent to produce rGO sheets from oxidized graphite.

Hydrothermal route has been employed for transformation of carbohydrate molecules to form homogeneous carbon nanospheres and nanotubes in many studies^{69, 70}, and also often been employed to reduce the oxygen-containing functional groups on GO to restore the basal plane

carbon structure of graphene⁷¹⁻⁷⁵. Superheated water with high temperature and high pressure is also confirmed to possess reducing ability and offers a green chemistry alternative to toxic reducing agent. Metal particles have been successfully reduced from metal oxides or metal salts in SC H₂O⁷⁶⁻⁷⁸. Therefore, SCFs process may be a plausible reduction method to produce rGO sheets by removing oxygen functional groups from GO planar and repairing the aromatic structures^{72, 79, 80}.

Khatri's group thoroughly investigated the controlled deoxygenation of GO in sub/supercritical H₂O without adding other reducing agent. They found that compared to that of at moderate temperature (373 K), the degree of deoxygenation was found to be higher and the p-conjugated network in the hydrothermally treated samples was better restored at the high temperature (473–653 K). The hydrogen ion initiated dehydration by inter- or intramolecular reactions, reduction of highly strained epoxide groups, decarboxylation and generation of conjugated p-network is considered to be the plausible mechanism for deoxygenation of GO under hydrothermal conditions on the basis of spectroscopic results⁸¹.

Different from SC CO₂ and SC H₂O, SC alcohols can donate hydrogen in the form of molecular hydrogen, hydride, or protons, which make it a more efficient reducing agent to produce metal particles⁸²⁻⁸⁴, hydrogenation of double bonds in organic compounds and the reduction of aldehydes and ketones to their corresponding alcohols⁸⁵. Kim's group compared the reduction performance of four different SC alcohols to clarify the mechanism of SC alcohols reduction. They suggested that the deoxygenation of GO in SC alcohols proceeds through thermal and chemical routes. The liquid and gas product analysis after the SC EtOH reduction revealed that the dominant chemical de-epoxidation routes are hydrogen donation followed by dehydration^{86, 87}.

Bao and co-workers produced GO paper using SC EtOH. As a sole component of the anode in lithium ion batteries, the production's specific capacity was comparable to those of free standing GO papers reduced by hydrazine or carbon nanotube paper⁸⁸. Sun's group also confirm the excellent reduction ability of SC EtOH. They found that the restored electrical conductivity compares favorably to those for rGO from many other conversion approaches, only except for a few that require thermal annealing at very high temperature⁸⁹. Honma's group use platelet carbon nanofibers as starting material to produce nanographene in SC EtOH. Raman results indicated that the defects in platelet carbon nanofibers were significantly reduced during SCFs reaction⁶⁵.

4. Concluding remarks

Using SCFs intercalation and exfoliation method to produce graphene is an extension of liquid exfoliation. Pretreatment of graphite chunk, intercalation and exfoliation are the three stages of this approach, the pretreatment step affects the intercalation degree of SCFs, and the intercalation degree of SCFs has great impact on the exfoliation efficiency of the following exfoliation step. Although graphene sheets can be directly exfoliated from pristine graphite crystal by SCFs, slightly oxidized graphite and expandable graphite can increase the ratio of monolayer graphene sheets in final products. In SCFs intercalation step, SCFs penetrate into graphite chunk to form a layer of agent and expand the distance between carbon layers. Choosing appropriate SCFs media, using ultrasonic or stirring assistance and adding molecular wedge can promote the intercalation extent. In the next exfoliation step, rapid expansion is the common method to exfoliate graphene sheets from intercalated graphite, ultrasonic cavitation and jet cavitation can strengthen the efficiency of exfoliation by cavitation. Besides SCFs intercalation and exfoliation method, SCFs process is also considered as a plausible reduction method to produce rGO sheets

by removing oxygen functional groups from GO planar and repairing the aromatic structures. ccc

In SCFs intercalation and exfoliation approach, the electrical and thermal properties of graphene can be kept well owing to the directly exfoliation from graphite using fluids. Both graphene powder and graphene dispersion can be obtained to meet a variety of application needs. Additives can be easily added in reaction system to synthesize graphene-based composite materials. Using SCFs technology to produce graphene allows us to develop a continuous-flow-type reactor system to produce graphene in large-scale with low-cost. Since low-cost and large-scale production are two major obstacles restricting the commercialization of graphene, SCFs producing route may become a very promising commercial technology to produce graphene, and will greatly reduce the cost in applications such as battery, conductive polymer, conductive ink etc., in which large quantities of highly conductive graphene are needed.

Acknowledgments

We gratefully acknowledge financial support by the National Natural Science Foundation of China (15Z103150042) and China Postdoctoral Science Foundation (15Z102060007).

References

1. M. V. Bracamonte, G. I. Lacconi, S. E. Urreta and L. E. F. Foa Torres, *J. Phys. Chem. C*, 2014, 118, 15455-15459.
2. Y. L. Zhong, Z. Tian, G. P. Simon and D. Li, *Materials Today*, 2015, 18, 73-78.
3. Y. Hernandez, V. Nicolosi, M. Lotya, F. M. Blighe, Z. Sun, S. De, I. T. McGovern, B. Holland, M. Byrne, Y. K. Gun'Ko, J. J. Boland, P. Niraj, G. Duesberg, S. Krishnamurthy, R. Goodhue, J. Hutchison, V. Scardaci, A. C. Ferrari and J. N. Coleman, *Nat. Nano*, 2008, 3, 563-568.
4. Y. Arao and M. Kubouchi, *Carbon*, 2015, 95, 802-808.
5. S. K. Goel and E. J. Beckman, *Polymer Engineering & Science*, 1994, 34, 1137-1147.
6. DeSimone and J. M., *Science*, 2002, 297, 799-803.
7. Q. D. Truong, M. K. Devaraju, Y. Ganbe, T. Tomai and I. Honma, *Sci. Rep.*, 2014, 4.
8. G. K. Serhatkulu, C. Dilek and E. Gulari, *J. Supercrit. Fluid*, 2006, 39, 264-270.
9. K. P. Johnston and P. S. Shah, *Science*, 2004, 303, 482-483.
10. K. Jang, J. Lee, I.-K. Hong and S. Lee, *Korea-Aust. Rheol. J.*, 2013, 25, 145-152.
11. M. R. Thompson, Z. Zhuang, J. Liu and W. R. Rodgers, *Polym. Eng. Sci.*, 2012, 52, 2049-2062.
12. G. Hu, L. Yi and C. Liu, *J. Supercrit. Fluid*, 2012, 72, 59-67.
13. E. Akbarinezhad, M. Ebrahimi and F. Sharif, *J. Supercrit. Fluid*, 2011, 59, 124-130.
14. *US Pat.*, US7157517B2, 2007.
15. Y. Lee, S. Kim, H.-i. Lee, H. Jeong, A. Raghu, K. Reddy and B. Kim, *Macromol. Res.*, 2011, 19, 66-71.
16. K. R. Reddy, M. Hassan and V. G. Gomes, *Appl. Catal. A-Gen.*, 2015, 489, 1-16.
17. S. Stankovich, D. A. Dikin, R. D. Piner, K. A. Kohlhaas, A. Kleinhammes, Y. Jia, Y. Wu, S. T. Nguyen and R. S. Ruoff, *Carbon*, 2007, 45, 1558-1565.
18. S. H. Choi, D. H. Kim, A. V. Raghu, K. R. Reddy, H.-I. Lee, K. S. Yoon, H. M. Jeong and B. K. Kim, *J. Macromol. Sci. B*, 2012, 51, 197-207.
19. M. Hassan, E. Haque, K. R. Reddy, A. I. Minett, J. Chen and V. G. Gomes, *Nanoscale*, 2014, 6, 11988-11994.
20. V. León, A. M. Rodríguez, P. Prieto, M. Prato and E. Vázquez, *ACS Nano*, 2014, 8, 563-571.
21. M.-T. Lee, C.-Y. Fan, Y.-C. Wang, H.-Y. Li, J.-K. Chang and C.-M. Tseng, *J. Mater. Chem. A*, 2013, 1, 3395-3405.
22. J. Zhao, H. Xue, L. Zhang, J. Yu and H. Hu, *J. Nanopart. Res.*, 2012, 14, 1-11.
23. J. Zhao, Z. Liu, Y. Qin and W. Hu, *CrystEngComm*, 2014, 16, 2001-2008.
24. K. Mase, H. Kondo, S. Kondo, M. Hori, M. Hiramatsu and H. Kano, *Appl. Phys. Lett.*, 2011, 98, 193108.
25. F. Nasrin, M.-G. Yaocihuatl, C. Rajib Roy and A. C. Paul, *Nanotechnology*, 2012, 23, 294005.
26. D.-H. Jiang, C.-H. Yang, C.-M. Tseng, S.-L. Lee and J.-K. Chang, *Nanoscale*, 2014, 6, 12565-12572.
27. J. Zhao, L. Zhang, H. Xue, Z. Wang and H. Hu, *RSC Adv.*, 2012, 2, 9651-9659.
28. Y. Haldorai, W. Voit and J.-J. Shim, *Electrochim. Acta*, 2014, 120, 65-72.
29. J. Zhao, L. Zhang, T. Chen, H. Yu, L. Zhang, H. Xue and H. Hu, *J. Phys. Chem. C*, 2012, 116, 21374-21381.
30. J. Zhao, H. Yu, Z. Liu, M. Ji, L. Zhang and G. Sun, *J. Phys. Chem. C*, 2014, 118, 1182-1190.
31. Y. Haldorai and J.-J. Shim, *Mater. Lett.*, 2014, 133, 24-27.

32. C.-H. Wu, C.-H. Wang, M.-T. Lee and J.-K. Chang, *J. Mater. Chem.*, 2012, 22, 21466-21471.
33. N. Farhangi, R. R. Chowdhury, Y. Medina-Gonzalez, M. B. Ray and P. A. Charpentier, *Appl. Catal. B-Environ.*, 2011, 110, 25-32.
34. M. Sathish, S. Mitani, T. Tomai and I. Honma, *J. Mater. Chem. A*, 2014, 2, 4731-4738.
35. W. Qian, X. Cui, R. Hao, Y. Hou and Z. Zhang, *ACS Appl. Mater. Inter.*, 2011, 3, 2259-2264.
36. S. S. Balaji and M. Sathish, *RSC Adv.*, 2014, 4, 52256-52262.
37. A. Hadi, J. Karimi-Sabet, S. M. A. Moosavian and S. Ghorbanian, *J. Supercrit. Fluid*, 2016, 107, 92-105.
38. C. Wattanaprayoon, Master Thesis, Michigan Technological University, 2011.
39. D. Rangappa, K. Sone, M. Wang, U. K. Gautam, D. Golberg, H. Itoh, M. Ichihara and I. Honma, *Chem. - Eur. J.*, 2010, 16, 6488-6494.
40. C. Liu and G. Hu, *Ind. Eng. Chem. Res.*, 2014, 53, 14310-14314.
41. Jose L. Gomez-Ballesteros, Alejandro Callejas-Tovar, Luiz A. F. Coelho and P. B. Balbuena, in *Design and applications of nanomaterials for devices and sensors*, ed. J. M. Seminario, Springer Netherlands, 2014, DOI: 10.1007/978-94-017-8848-9, ch. 6, pp. 171-184.
42. C. Liu, G. Hu and H. Gao, *J. Supercrit. Fluid*, 2012, 63, 99-104.
43. M. Hassan, K. R. Reddy, E. Haque, A. I. Minett and V. G. Gomes, *J. Colloid Interf. Sci.*, 2013, 410, 43-51.
44. R. Zhang, B. Zhang and S.-Q. Sun, *RSC Adv.*, 2015, 5, 44783-44791.
45. J.-H. Jang, D. Rangappa, Y.-U. Kwon and I. Honma, *J. Mater. Chem.*, 2011, 21, 3462-3466.
46. Y. Gao, W. Shi, W. Wang, Y. Wang, Y. Zhao, Z. Lei and R. Miao, *Ind. Eng. Chem. Res.*, 2014, 53, 2839-2845.
47. B. Wu and X. Yang, *J. Colloid Interf. Sci.*, 2011, 361, 1-8.
48. W. Wang, Y. Wang, Y. Gao and Y. Zhao, *J. Supercrit. Fluid*, 2014, 85, 95-101.
49. N.-W. Pu, C.-A. Wang, Y. Sung, Y.-M. Liu and M.-D. Ger, *Mater. Lett.*, 2009, 63, 1987-1989.
50. H. S. Sim, T. A. Kim, K. H. Lee and M. Park, *Mater. Lett.*, 2012, 89, 343-346.
51. Y. P. Zhang, S. H. Lee, K. R. Reddy, A. I. Gopalan and K. P. Lee, *J. Appl. Polym. Sci.*, 2007, 104, 2743-2750.
52. L. Li, J. Xu, G. Li, X. Jia, Y. Li, F. Yang, L. Zhang, C. Xu, J. Gao, Y. Liu and Z. Fang, *Chem. Eng. J.*, 2016, 284, 78-84.
53. X. Zheng, Q. Xu, J. Li, L. Li and J. Wei, *RSC Adv.*, 2012, 2, 10632-10638.
54. L. Li, X. Zheng, J. Wang, Q. Sun and Q. Xu, *ACS Sustain. Chem. Eng.*, 2012, 1, 144-151.
55. S. Xu, Q. Xu, N. Wang, Z. Chen, Q. Tian, H. Yang and K. Wang, *Chem. Mater.*, 2015, 27, 3262-3272.
56. C. Zhang, W. Lv, X. Xie, D. Tang, C. Liu and Q.-H. Yang, *Carbon*, 2013, 62, 11-24.
57. A. V. Tamashauskyy, *Am. Ceram. Soc. Bull.*, 1998, 77, 102-104.
58. Y.-T. Shieh, J.-G. Lai, W.-L. Tang, C.-H. Yang and T.-L. Wang, *J. Supercrit. Fluid*, 2009, 49, 385-393.
59. K. B. Bader, J. L. Raymond, J. Mobley, C. C. Church and D. Felipe Gaitan, *J. Acoust. Soc. Am.*, 2012, 132, 728-737.
60. K. B. Bader, J. Mobley, C. C. Church and D. F. Gaitan, *J. Acoust. Soc. Am.*, 2012, 132, 2286-2291.
61. A. Ciesielski and P. Samori, *Chem. Soc. Rev.*, 2014, 43, 381-398.
62. V. Štengl, *Chem. - Eur. J.*, 2012, 18, 14047-14054.

63. S. Zhigang, L. Jinzhi, Y. Min, Z. Xiaojing and M. Shulin, *Nanotechnology*, 2011, 22, 365306.
64. M. Yi, Z. Shen and J. Zhu, *Chin. Sci. Bull.*, 2014, 59, 1794-1799.
65. T. Tomai, Y. Kawaguchi and I. Honma, *Appl. Phys. Lett.*, 2012, 100, 233110.
66. T. Tomai, N. Tamura and I. Honma, *ACS Macro Lett.*, 2013, 2, 794-798.
67. P. J. Yunker, T. Still, M. A. Lohr and A. G. Yodh, *Nature*, 2011, 476, 308-311.
68. H. Gao, W. Shangguan, G. Hu and K. Zhu, *Appl. Catal. B-Environ.*, 2016, 180, 416-423.
69. C. Yao, Y. Shin, L.-Q. Wang, C. F. Windisch, W. D. Samuels, B. W. Arey, C. Wang, W. M. Risen and G. J. Exarhos, *J. Phys. Chem. C*, 2007, 111, 15141-15145.
70. X. Sun and Y. Li, *Angew. Chem. Int. Edit.*, 2004, 43, 597-601.
71. H. P. Mungse, O. P. Sharma, H. Sugimura and O. P. Khatri, *RSC Adv.*, 2014, 4, 22589-22595.
72. Y. Zhou, Q. Bao, L. A. L. Tang, Y. Zhong and K. P. Loh, *Chem. Mater.*, 2009, 21, 2950-2956.
73. D. Long, W. Li, L. Ling, J. Miyawaki, I. Mochida and S.-H. Yoon, *Langmuir*, 2010, 26, 16096-16102.
74. L. Sun, L. Wang, C. Tian, T. Tan, Y. Xie, K. Shi, M. Li and H. Fu, *RSC Adv.*, 2012, 2, 4498-4506.
75. S. D. Perera, R. G. Mariano, K. Vu, N. Nour, O. Seitz, Y. Chabal and K. J. Balkus Jr, *ACS Catal.*, 2012, 2, 949-956.
76. J.-Y. Chang, J.-J. Chang, B. Lo, S.-H. Tzing and Y.-C. Ling, *Chem. Phys. Lett.*, 2003, 379, 261-267.
77. K. J. Ziegler, R. C. Doty, K. P. Johnston and B. A. Korgel, *J. Am. Chem. Soc.*, 2001, 123, 7797-7803.
78. K. Sue, A. Suzuki, M. Suzuki, K. Arai, Y. Hakuta, H. Hayashi and T. Hiaki, *Ind. Eng. Chem. Res.*, 2006, 45, 623-626.
79. J. Shen, B. Yan, M. Shi, H. Ma, N. Li and M. Ye, *J. Mater. Chem.*, 2011, 21, 3415-3421.
80. G.-J. Liu, L.-Q. Fan, F.-D. Yu, J.-H. Wu, L. Liu, Z.-Y. Qiu and Q. Liu, *J. Mater. Sci.*, 2013, 48, 8463-8470.
81. H. P. Mungse, O. P. Sharma, H. Sugimura and O. P. Khatri, *RSC Adv.*, 2014, 4, 22589-22595.
82. H. Choi, B. Veriansyah, J. Kim, J.-D. Kim and J. W. Kang, *J. Supercrit. Fluid*, 2010, 52, 285-291.
83. J. Kim, D. Kim, B. Veriansyah, J. Won Kang and J.-D. Kim, *Mater. Lett.*, 2009, 63, 1880-1882.
84. S. P. Gubin and E. Y. Buslaeva, *Russ. J. Phys. Chem. B*, 2009, 3, 1172-1186.
85. T. Nakagawa, H. Ozaki, T. Kamitanaka, H. Takagi, T. Matsuda, T. Kitamura and T. Harada, *J. Supercrit. Fluid*, 2003, 27, 255-261.
86. E. Budi Nursanto, A. Nugroho, S.-A. Hong, S. J. Kim, K. Yoon Chung and J. Kim, *Green Chem.*, 2011, 13, 2714-2718.
87. M. Seo, D. Yoon, K. S. Hwang, J. W. Kang and J. Kim, *Carbon*, 2013, 64, 207-218.
88. S. Liu, K. Chen, Y. Fu, S. Yu and Z. Bao, *Appl. Surf. Sci.*, 2012, 258, 5299-5303.
89. C. Y. Kong, W.-L. Song, M. J. Meziani, K. N. Tackett li, L. Cao, A. J. Farr, A. Anderson and Y.-P. Sun, *J. Supercrit. Fluid*, 2012, 61, 206-211.

Graphical Abstract

